EUROPEAN ORGANIZATION FOR NUCLEAR RESEARCH (CERN)

Measurement of the mass difference and relative production rate of the Ω_b^- and Ξ_b^- baryons

LHCb collaboration[†]

Abstract

The mass difference between the Ω_b^- and Ξ_b^- baryons is measured using proton-proton collision data collected by the LHCb experiment, corresponding to an integrated luminosity of $9\,\text{fb}^{-1}$, and is found to be

$$m(\Omega_b^-) - m(\Xi_b^-) = 248.54 \pm 0.51\,(\text{stat}) \pm 0.38\,(\text{syst})\,\text{MeV}/c^2.$$

The mass of the Ω_b^- baryon is measured to be

$$m(\Omega_b^-) = 6045.9 \pm 0.5\,(\text{stat}) \pm 0.6\,(\text{syst})\,\text{MeV}/c^2.$$

This is the most precise determination of the Ω_b^- mass to date. In addition, the production rate of Ω_b^- baryons relative to that of Ξ_b^- baryons is measured for the first time in pp collisions, using an LHCb dataset collected at a center-of-mass energy of $13\,\text{TeV}$ and corresponding to an integrated luminosity of $6\,\text{fb}^{-1}$. Reconstructing beauty baryons in the kinematic region $2 < \eta < 6$ and $p_T < 20\,\text{GeV}/c$ with their decays to a J/ψ meson and a hyperon, the ratio

$$\frac{f_{\Omega_b^-}}{f_{\Xi_b^-}} \times \frac{\mathcal{B}(\Omega_b^- \to J/\psi\,\Omega^-)}{\mathcal{B}(\Xi_b^- \to J/\psi\,\Xi^-)} = 0.120 \pm 0.008\,(\text{stat}) \pm 0.008\,(\text{syst}),$$

is obtained, where $f_{\Omega_b^-}$ and $f_{\Xi_b^-}$ are the fragmentation fractions of b quarks into Ω_b^- and Ξ_b^- baryons, respectively, and $\mathcal{B}$ represents the branching fractions of their respective decays.

[†]Authors are listed at the end of this paper.

1   Introduction

The quark model predicts fifteen b-baryon states, containing one b quark and two lighter quarks (u, d or s), that are neither orbitally nor radially excited. Four of these states, namely Λ_b^0, Ξ_b^0, Ξ_b^- and Ω_b^-, are particularly interesting since they can only decay through the weak interaction, leading to lifetimes of about 1.5 ps [1]. Due to the relatively high masses of the b baryons, currently only high-energy accelerators such as the Large Hadron Collider (LHC) copiously produce all their types. As a consequence, the current experimental knowledge on the b-baryon mass hierarchy, properties and decay modes is limited mainly to the results of hadron-collider experiments.

The heaviest of the four weakly decaying baryons, the Ω_b^- state with ssb quark content in the constituent quark model, is the least-well studied. While both the DØ and CDF collaborations claimed the observation of the $\Omega_b^- \to J/\psi \Omega^-$ decay, the reported mass values, $6165 \pm 10\,(\text{stat}) \pm 13\,(\text{syst})\,\text{MeV}/c^2$ by DØ [2] and $6054.4 \pm 6.8\,(\text{stat}) \pm 0.9\,(\text{syst})\,\text{MeV}/c^2$ by CDF [3], differ by more than six standard deviations. The situation was clarified by the LHCb experiment in 2013 [4] with the confirmation of the state observed by CDF using the same decay mode. In 2014, the CDF experiment observed a second decay mode, $\Omega_b^- \to \Omega_c^0 \pi^-$ [5], confirmed by LHCb in 2016 [6]. Both CDF and LHCb have measured the mass and lifetime of the Ω_b^- baryon. However, in both cases the measurements were limited by the available datasets having yields as low as a few tens of signal candidates. Recently, LHCb published a more precise measurement of the Ω_b^- baryon mass via its decay mode $\Omega_b^- \to \Xi_c^+ K^- \pi^-$ [7].

This paper presents a measurement of the Ω_b^- baryon mass with the $\Omega_b^- \to J/\psi \Omega^-$ decay (charge conjugation is implied throughout this paper), using the full LHCb proton-proton (pp) collision dataset collected from 2011 to 2018, corresponding to an integrated luminosity of $9\,\text{fb}^{-1}$, at center-of-mass energies of $7, 8$ and $13\,\text{TeV}$. Reconstructing the Ω_b^- baryon through the decay chain $\Omega_b^- \to J/\psi \Omega^-$, $\Omega^- \to \Lambda K^-$ and $\Lambda \to p\pi^-$ is particularly advantageous since the cascade topology of the decay of two long-lived hyperons cannot be mimicked by any mesonic decay. This final state leads to very clean signal samples and therefore is well suited for a mass measurement.

This paper also presents the first measurement of the relative production rates of the Ω_b^- and Ξ_b^- baryons at the LHC, in pp collisions at a center-of-mass energy of $13\,\text{TeV}$, using a dataset corresponding to an integrated luminosity of $6\,\text{fb}^{-1}$. In order to measure the absolute branching fractions of Ω_b^- decays at the LHC, it is necessary to consider the probability of the b-quark hadronization into the Ω_b^- baryon, denoted as $f_{\Omega_b^-}$, in proton-proton collisions. This quantity is also required to measure the total b-quark production cross-section at the LHC, but until now only phenomenological estimates were available [8]. Experimentally, the quantity accessible at the LHC is the product of the production rate of a baryon and the branching fraction of its decay to a specific final state. This makes it difficult to measure the absolute production rates or absolute branching fractions at hadron colliders without external input. For the Λ_b^0 baryon, the production rate was measured at LHCb relative to B mesons. The most precise measurement utilizes the predicted similarity of b-hadron semileptonic decay widths [9]. At the moment, extending this technique to the Ω_b^- baryon is not possible: although semileptonic decays of Ω_b^- have been used by LHCb to obtain a sample of Ω_c^0 baryons [10], the absolute branching fractions for the Ω_c^0 decays are not known [1].

The CDF experiment has measured the relative production rates of the Ω_b^-, Λ_b^0 and Ξ_b^-

baryons multiplied by their relative decay rates to the final states with a J/ψ meson and a hyperon, in $p\bar{p}$ collisions at the center-of-mass energy of 1.96 TeV at the Tevatron [3].[1] Since the Tevatron and the LHC use different colliding particles and center-of-mass energies, it is necessary to perform an independent measurement of the relative production fraction at the LHC. The decays $\Omega_b^- \to J/\psi\Omega^-$ and $\Xi_b^- \to J/\psi\Xi^-$ are well suited to perform such a measurement, given their similar topologies and final-state particles. Unfortunately, the relative production fractions cannot be disentangled from the ratio of branching fractions due to the limited knowledge of the absolute branching fractions of the chosen decays or their ratio. Therefore, the relative production rate of the Ω_b^- and Ξ_b^- baryons is determined with the ratio

$$R \equiv \frac{f_{\Omega_b^-}}{f_{\Xi_b^-}} \times \frac{\mathcal{B}(\Omega_b^- \to J/\psi\Omega^-)}{\mathcal{B}(\Xi_b^- \to J/\psi\Xi^-)}. \tag{1}$$

In the past, LHCb has used a similar approach to measure the relative production rate of the Ξ_b^- and Λ_b^0 baryons [11] using their decays $\Xi_b^- \to J/\psi\Xi^-$ and $\Lambda_b^0 \to J/\psi\Lambda$. These two decay modes are linked by an SU(3) symmetry, which simplifies the theoretical interpretation of this measurement in terms of $f_{\Xi_b^-}/f_{\Lambda_b^0}$. There is no such symmetry relation between the $\Omega_b^- \to J/\psi\Omega^-$ and $\Xi_b^- \to J/\psi\Xi^-$ decays that can be used to determine $f_{\Omega_b^-}/f_{\Xi_b^-}$, because the Ω^- baryon is not a member of the same baryon multiplet as the Ξ^- and Λ baryons. Therefore, further theoretical input is needed to directly access the production ratio $f_{\Omega_b^-}/f_{\Xi_b^-}$. Predictions of branching fractions of the $\Omega_b^- \to J/\psi\Omega^-$ and $\Xi_b^- \to J/\psi\Xi^-$ decays have been obtained, among others, with the nonrelativistic quark model [12], covariant confined quark model [13], and light-front quark model [14] approaches. The lack of consistency among the different models requires further study. Therefore, the primary quantity measured in this paper is the ratio defined in Eq. (1).

This paper is organized as follows: after a short introduction of the LHCb detector and its data processing chain in Sec. 2, the candidate selection and background suppression is described in Sec. 3. The mass measurement is described in Sec. 4 and the relative production rate measurement in Sec. 5. This paper concludes with a discussion of the results in Sec. 6.

2 LHCb detector and datasets

The LHCb detector [15, 16] is a single-arm forward spectrometer covering the pseudorapidity range $2 < \eta < 5$, designed for the study of particles containing b or c quarks. The detector includes a high-precision tracking system consisting of a silicon-strip vertex detector (VELO) surrounding the pp interaction region [17], a large-area silicon-strip detector located upstream of a dipole magnet with a bending power of about 4 Tm, and three stations of silicon-strip detectors and straw drift tubes [18, 19] placed downstream of the magnet. The tracking system provides a measurement of the momentum, p, of charged particles with a relative uncertainty that varies from 0.5% at low momentum to 1.0% at 200 GeV/c. The minimum distance of a track to a primary pp collision vertex (PV), the impact parameter (IP), is measured for charged particles

---

[1]A similar measurement was also performed by the DØ experiment [2], but since the mass value of the state observed by DØ is incompatible with other experiments, this result is omitted.

reconstructed in all tracking subdetectors with a resolution of $(15 + 29/p_{\mathrm{T}})\,\upmu\mathrm{m}$, where p_{T} is the component of the momentum transverse to the beam, in GeV/c. Different types of charged hadrons are distinguished using information from two ring-imaging Cherenkov detectors [20]. Muons are identified by a system composed of alternating layers of iron and multiwire proportional chambers [21].

The datasets considered for this measurement were collected by LHCb between 2011-2012 at center-of-mass energies of 7 and 8 TeV (Run 1), corresponding to an integrated luminosity of $3\,\mathrm{fb}^{-1}$, and between 2015-2018 at a center-of-mass energy of 13 TeV (Run 2), corresponding to an integrated luminosity of $6\,\mathrm{fb}^{-1}$. For the relative production rate measurement, only the Run 2 dataset is used, where the simulated samples describe the reconstruction of long-lived hyperons more precisely. The online event selection is performed by a trigger [22], which consists of a hardware stage, based on information from the calorimeters and the muon system, followed by a software stage, which applies a full event reconstruction. At the hardware stage, the event is required to have a muon with a high transverse momentum or a dimuon pair with a high product of transverse momenta of the two muons. At the software stage, the dimuon pair must have a significant displacement from the PV.

The momentum scale is calibrated using samples of $J/\psi \rightarrow \mu^+\mu^-$ and $B^+ \rightarrow J/\psi K^+$ decays collected concurrently with the data sample used for this analysis [4,23]. A relative uncertainty of 3×10^{-4} is estimated using samples of other fully reconstructed b hadrons, Υ mesons and K_{S}^0 mesons.

Simulated samples of $\Omega_b^- \rightarrow J/\psi\,\Omega^-$ and $\Xi_b^- \rightarrow J/\psi\,\Xi^-$ decays are used to model detector effects and selection requirements. In the simulation, pp collisions are generated using PYTHIA [24] with a specific LHCb configuration [25]. As the Ω_b^- production rate in PYTHIA is very low, its generation is inefficient. Therefore, the Ω_b^- baryon is simulated as a Ξ_b^- baryon with the mass and lifetime values altered to match the Ω_b^- world-average values. Decays of unstable particles are described by EvtGen [26], in which final-state radiation is generated using PHOTOS [27]. The decays of the Ω_b^- and Ξ_b^- baryons are simulated according to available phase space. The decays of the Ω^-, Ξ^- and Λ hyperons are simulated with a dedicated helicity-amplitude model, using the latest world-average values of parity-violating asymmetry parameters in these decays [1]. The interaction of the generated particles with the LHCb detector, and its response, are implemented using the GEANT4 toolkit [28] as described in Ref. [29].

3 Candidate selection

The decays $\Omega_b^- \rightarrow J/\psi\,\Omega^-$ and $\Xi_b^- \rightarrow J/\psi\,\Xi^-$ share a particular topology, which is distinct from most other processes occurring in the LHCb detector. The cascade topology of the $\Xi^- \rightarrow \Lambda[\rightarrow p\pi^-]\pi^-$ and $\Omega^- \rightarrow \Lambda[\rightarrow p\pi^-]K^-$ decays cannot be produced by any meson decays and provides a clean signature for hyperon decays at LHCb. This feature is exploited in the design of the selection requirements used in this analysis.

In this paper, reconstructed charged hadrons are classified into two categories. The *long-track* category (L) refers to tracks that have reconstructed segments in both the VELO and the subsequent tracking stations. The *downstream-track* category (D) consists of particles with trajectories that are not reconstructed in the VELO, and only include information from the tracking detectors just before and after the LHCb magnet. While

most of the reconstructed charged particles produced in the pp collisions form long tracks, the decay products of long-lived hyperons tend to be reconstructed as downstream tracks. Due to the presence of tracking information from the VELO detector, the trajectories, and hence the IP, of long tracks are measured with better precision than those of downstream tracks. Since the Ω^- and Ξ^- baryons are long lived and their decay products include another long-lived particle, the Λ hyperon, the majority of the signal candidates have at least two downstream tracks.

Signal Ω_b^- and Ξ_b^- candidates are built by combining an Ω^- or Ξ^- hyperon candidate, respectively, with a J/ψ meson candidate. The J/ψ candidate is reconstructed from two oppositely charged particles that are reconstructed as long tracks, are identified as muons by the muon system and are assigned a muon mass hypothesis. The dimuon invariant mass is required to be within the range 3000–3150 MeV/c^2. The Ω^- candidates are reconstructed via the ΛK^- decay mode, while the Ξ^- candidates are reconstructed via the $\Lambda \pi^-$ decay mode. The Λ hyperon candidate is built from a pair of oppositely charged particles, both forming either long or downstream tracks, that are assigned the proton and pion hypotheses, and originate from a common displaced vertex. The Λ candidate is subsequently combined with a displaced charged particle, which is reconstructed as either a long or a downstream track, and is assigned a kaon (for the Ω^-) or a pion (for the Ξ^-) mass hypothesis. As a result, the Ξ^- and Ω^- hyperons can be reconstructed in three track-type categories: LLL, where the kaon (pion) of the Ω^- (Ξ^-) decay, and the pion and proton of the Λ decay are all reconstructed from long tracks; LDD, where the Λ decay products are reconstructed from downstream tracks; and DDD, where all the hyperon decay products are reconstructed from downstream tracks. The proportion of the LLL and LDD categories is larger in the Ω_b^- decay than in the Ξ_b^- decay, due to the lifetime of the Ω^- hyperon being about half of the Ξ^- lifetime.

The Ω^-, Ξ^- and Λ candidates are required to have a decay vertex of good quality and a decay time greater than 2 ps. The Λ candidate must have an invariant mass within 8 MeV/c^2 around the known Λ baryon mass [1]. The Ω^- and Ξ^- candidates are required to have an invariant mass within 10 MeV/c^2 around their known world-average values [1], where the mass of the Λ candidate is constrained to its world-average value. Together, all these requirements preserve more than 90% of reconstructed signal candidates in both channels. To further suppress the background, the Ω^- and Ξ^- hyperons are both required to have $p_{\rm T}$ above 1 GeV/c; this requirement preserves about 93% of signal candidates in each decay mode. The Ω_b^- and Ξ_b^- candidates are also required to form a good vertex which is significantly displaced from the PV, and their momentum vectors must be consistent with originating from the PV. Since the Ξ_b^- decay includes two pions, it is ensured that the two pion tracks are not duplicates reconstructed from the same particle. This is done by requiring the angle between the two pions in the laboratory frame to be greater than 0.5 mrad. This requirement preserves more than 99% of signal and for consistency, is also applied between the kaon and pion tracks of the Ω^- decay.

For the $\Xi_b^- \to J/\psi \Xi^-$ decay, the background of $\Lambda_b^0 \to J/\psi \Lambda$ decays combined with a random pion is an important contribution. This background can pollute the region below the signal peak, as $m(\Lambda_b^0) + m(\pi^-) < m(\Xi_b^-)$. However, for the Ω_b^- case with $m(\Lambda_b^0) + m(K^-) > m(\Omega_b^-)$ the equivalent background only contributes to the far upper sideband and can therefore be neglected. To suppress this background in the Ξ_b^- decays, the pion from the Ξ^- decay is required to have a significant displacement from the PV. The equivalent displacement requirement is applied to the kaon of the Ω^- decay to improve

the cancellation of systematic uncertainties. These requirements retain about 93% of signal candidates in each decay mode.

A possible source of background for $\Omega_b^- \to J/\psi\Omega^-$ decays are $\Xi_b^- \to J/\psi\Xi^-$ decays, where a pion is misidentified as a kaon. Conversely, in the $\Xi_b^- \to J/\psi\Xi^-$ case, the background with a kaon misidentified as a pion is negligible due to the low Ω_b^- production cross-section. A highly efficient way to suppress this background is by applying a strict kaon identification requirement to the kaon candidate. This approach is used for the mass measurement. However, a precise calibration of the efficiency for this requirement is difficult to perform when the kaon is reconstructed as a downstream track. Therefore, an alternative approach is used for the measurement of the relative production rate: the invariant mass of the ΛK^- combination is calculated under the pion mass hypothesis for the kaon, and the resulting Ξ^- mass peak is vetoed. This preserves about 97% of Ω_b^- candidates.

The contribution from partially reconstructed $\Xi_b \to J/\psi\Xi(1530)$ decays, where the $\Xi(1530)$ resonance decays to a $\Xi^-\pi$ final state, is expected to be negligible due to non-overlapping wave functions of the Ξ_b and $\Xi(1530)$ baryons [30]. Higher Ξ states, located above the ΛK threshold, have relatively small decay widths to the $\Xi^-\pi$ channel. These partially reconstructed processes fail the selection requirements of this measurement due to significant missing energy. Furthermore, all excited Ω^- states are located above the ΞK threshold [1,31] and have low partial widths for the $\Omega\gamma$ and isospin-violating $\Omega\pi^0$ decays. Therefore, no significant partially reconstructed background is expected in the two analyzed datasets.

The final states of interest can also be reached by Cabibbo-suppressed processes such as $\Xi_b^- \to J/\psi\Sigma(1385)^-$ and $\Omega_b^- \to J/\psi\Xi(1690)^-$, followed by strong decays such as $\Sigma(1385)^- \to \Lambda\pi^-$ and $\Xi(1690)^- \to \Lambda K^-$. Since the hadronic resonances produced in these decays are short-lived, these processes are suppressed by the displacement requirement applied on the hyperon candidates. Therefore, the dominant remaining background is combinatorial background, consisting mostly of J/ψ mesons combined with random tracks.

To improve the invariant-mass resolution, an additional kinematic fit is performed on each candidate [32], where the parent hadron is required to be consistent with originating from the primary vertex. Furthermore, the invariant masses of the J/ψ, Λ, Ξ^- and Ω^- candidates are constrained to their known mass values [1]. The resulting constrained invariant mass, m_{constr}, has a resolution around $5.4\,\mathrm{MeV}/c^2$ for the Ω_b^- decay and $6.0\,\mathrm{MeV}/c^2$ for the Ξ_b^- decay. The smaller invariant-mass resolution for the Ω_b^- decay, in comparison to the Ξ_b decay, is due to the lower energy release in this decay, as well as the lower lifetime of the Ω^- hyperon resulting in a higher proportion of long tracks, which have a better momentum resolution. Finally, to have a well-defined fiducial region, the Ω_b^- and Ξ_b^- candidates are required to have $2 < \eta < 6$ and $p_{\mathrm{T}} < 20\,\mathrm{GeV}/c$.

4 Measurement of the Ω_b^--baryon mass

The measurement of the Ω_b^--baryon mass is performed using an LHCb dataset of $9\,\mathrm{fb}^{-1}$. The collected data are considered separately for the Run 1 and Run 2 samples, which have slightly different invariant-mass resolutions. The mass difference $m(\Omega_b^-) - m(\Xi_b^-)$, rather than the absolute Ω_b^- mass, is extracted from an unbinned maximum-likelihood fit to benefit from canceling systematic uncertainties due to imprecise calibration of the

momentum scale. The fit is performed simultaneously to the two run periods and decay channels. It is implemented in the ROOFIT toolkit [33] within the ROOT framework [34].

The resulting invariant-mass spectra are shown in Fig. 1. Each signal parametrization is described by a linear combination of two double-sided Crystal Ball functions [35] with a common mean. The parameters of the signal component are determined from large samples of simulated signal decays; most of them are then fixed in fits to data. The remaining free parameters of the signal in the fit to data are the Ξ_b^- mass for both run periods, the mass difference $m(\Omega_b^-) - m(\Xi_b^-)$, the width of each signal peak, and the signal yields. The background is described in each dataset by an exponential function, with a freely varying normalization and slope. Table 1 shows the resulting signal yields in each dataset.

The mass difference from this fit is found to be

$$m(\Omega_b^-) - m(\Xi_b^-) = 248.60 \pm 0.51 \, (\text{stat}) \, \text{MeV}/c^2.$$
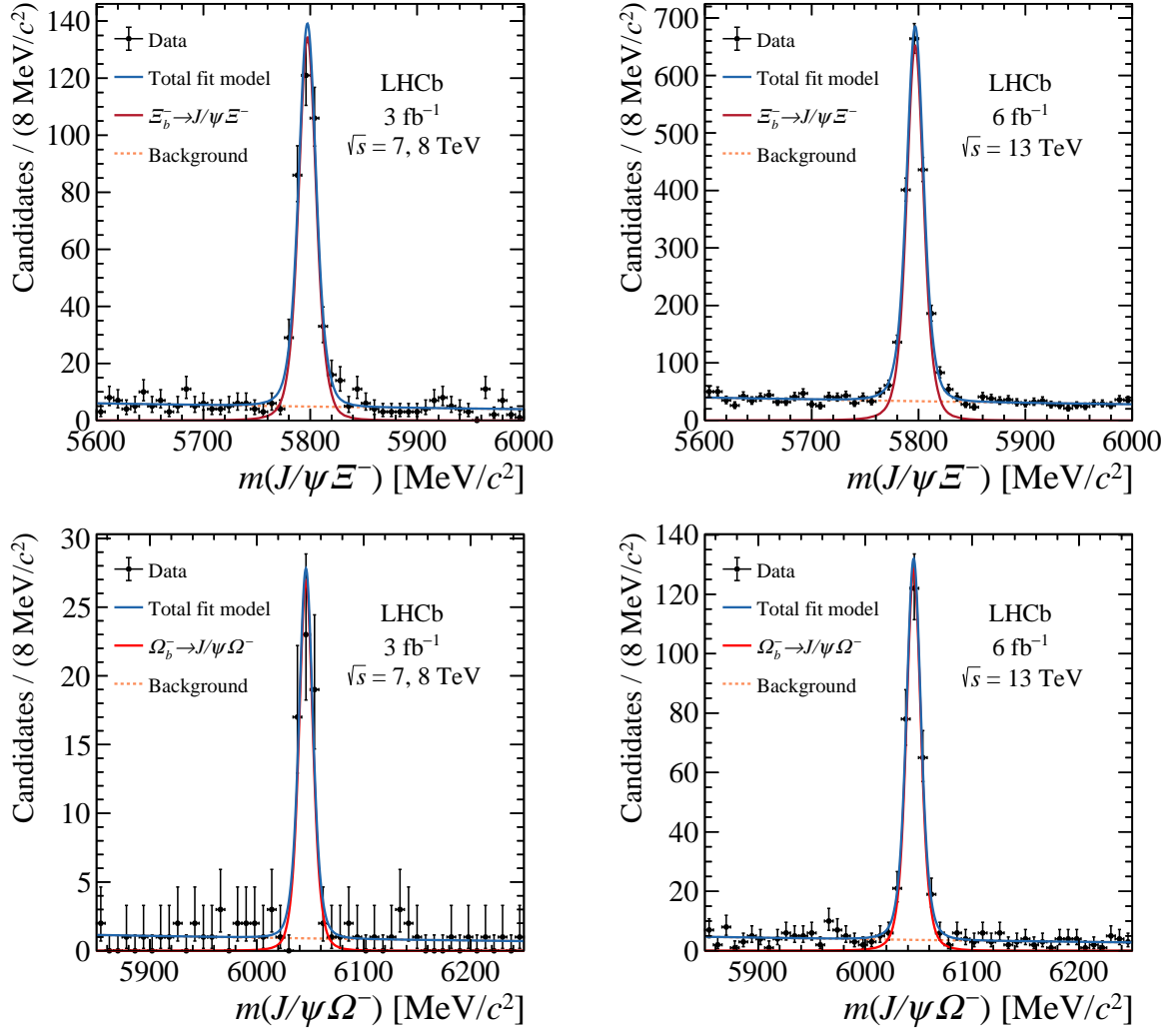
Figure 1: Invariant-mass distributions in the (top row) $\Xi_b^- \to J/\psi \Xi^-$ and (bottom row) $\Omega_b^- \to J/\psi \Omega^-$ datasets, in the (left column) Run 1 and (right column) Run 2 data-taking periods. The results of the simultaneous fit used for the mass-difference measurement are overlaid.

Table 1: Obtained values of signal yields from the fit to data.

Decay	Dataset	Signal yield
$\Xi_b^- \to J/\psi \Xi^-$	Run 1	377 ± 21
	Run 2	1790 ± 47
$\Omega_b^- \to J/\psi \Omega^-$	Run 1	60 ± 8
	Run 2	300 ± 18

To exclude dependencies of this result on the different data-taking periods and the track-type categories, the data sample is split into different subsets accordingly, and the mass-difference value measured for each subset. Furthermore, the analysed dataset is split by the charge of the b baryon, as well as by the magnet polarity with which the data was collected. Additional checks are performed by repeating the fit in a narrower invariant-mass range. All these cross-checks returned a mass difference in agreement with the baseline value, demonstrating the stability of this result.

The mass difference determined from the fit needs to be corrected for the positive bias $(0.06 \pm 0.02)\,\mathrm{MeV}/c^2$ observed from the fit to simulation. The uncertainty on this value is due to the size of the simulated sample. The final result therefore is corrected for the bias, and its absolute value is assigned as a systematic uncertainty. In order to access the final result and determine the value of the Ω_b^- mass, other sources of systematic uncertainty that do not cancel in the mass difference are studied. They are summarized in Table 2.

A variation of the momentum scale in simulation within its uncertainty of $\pm0.03\%$ leads to a systematic uncertainty of $0.09\,\mathrm{MeV}/c^2$ on the mass difference. The uncertainty on the amount of material assumed in the track reconstruction for the energy loss $(\mathrm{d}E/\mathrm{d}x)$ has been found to cancel up to $0.01\,\mathrm{MeV}/c^2$ in the measurements of mass differences, as long as the number of final-state tracks is the same between the two decay modes [4]. To propagate the uncertainty on the world-average values of the Ω^- and Ξ^- masses, the resulting bias on m_{constr} is estimated. This is performed by varying in simulated datasets the central values assumed in the mass constraints, according to their uncertainties. The average bias on the measured b-baryon mass is evaluated independently for the Ω_b^- and Ξ_b^- cases, by varying the value of the Ω^- and Ξ^- mass, respectively; the two uncertainties are then summed in quadrature. It is expected that the small uncertainties on the Λ and J/ψ mass values cancel in the mass difference. The resulting systematic uncertainty of $0.35\,\mathrm{MeV}/c^2$ is

Table 2: Systematic uncertainties on the mass-difference measurement. The total systematic uncertainty is obtained by summing all sources in quadrature.

Source	Uncertainty $[\,\mathrm{MeV}/c^2]$
Momentum scale	0.09
$\mathrm{d}E/\mathrm{d}x$ correction	0.01
Hyperon mass	0.35
$\Lambda_b^0 \to J/\psi \Lambda$ background	0.10
Fit bias	0.06
Full fit model	0.01
Total	0.38

dominated by the uncertainty of the Ω^- mass with $m_{\mathrm{PDG}}(\Omega^-) = 1672.45 \pm 0.29\,\mathrm{MeV}/c^2$ [1].

The systematic uncertainty associated to possible residual backgrounds from the $\Lambda_b^0 \to J/\psi\Lambda$ decay, combined with a random pion, is studied with four alternative approaches. These include three methods to suppress this background: applying a dedicated mass veto on the $J/\psi\Lambda$ invariant mass around the known Λ_b^0 mass value; requiring a large flight distance of the Ξ^- candidate; or rejection of good-quality $J/\psi\Lambda$ vertices. Alternatively, a dedicated component is included to account for this background in the fit. Averaging the resulting shifts from the baseline result leads to a systematic uncertainty of $0.10\,\mathrm{MeV}/c^2$ on the mass difference.

While for the signal model a fit bias of $0.06\,\mathrm{MeV}/c^2$ is observed, no significant additional bias is found for the full fit model. The systematic uncertainty related to the chosen fit model is assessed with pseudoexperiments for an alternative background model, where a linear parametrization is assumed instead of the exponential function, or an alternative signal model consisting of a single Crystal Ball distribution. The resulting combined uncertainty due to the fit model is $0.01\,\mathrm{MeV}/c^2$.

Correcting the mass difference for the value of the bias observed in the fit to simulation, and taking into account the systematic uncertainties, the mass difference is determined to be

$$m(\Omega_b^-) - m(\Xi_b^-) = 248.54 \pm 0.51\,(\mathrm{stat}) \pm 0.38\,(\mathrm{syst})\,\mathrm{MeV}/c^2.$$

The result is in agreement with the previous measurement by LHCb [6], but significantly more precise.

To obtain the value of $m(\Omega_b^-)$, the most precise measurement of the Ξ_b^- baryon mass to date is used: $m(\Xi_b^-) = 5797.33 \pm 0.24 \pm 0.29\,\mathrm{MeV}/c^2$ [36]. This measurement uses $\Xi_b^- \to \Xi_c^0\pi^-$ decays, and therefore is statistically independent of the $\Xi_b^- \to J/\psi\Xi^-$ dataset used in this paper. The systematic uncertainties are considered to be fully uncorrelated, except for the uncertainties due to momentum scale calibration and the energy loss correction, which are taken as fully correlated. This leads to a value of the Ω_b^- baryon mass of

$$m(\Omega_b^-) = 6045.9 \pm 0.5\,(\mathrm{stat}) \pm 0.6\,(\mathrm{syst})\,\mathrm{MeV}/c^2.$$

This value is the most precise determination of the Ω_b^- mass and is consistent with the current world average of $6045.2 \pm 1.2\,\mathrm{MeV}/c^2$ [1]. This result supersedes the value reported in Ref. [4].

Combining our value of $m(\Omega_b^-) - m(\Xi_b^-)$ with that in Ref. [6], and assuming that the systematic uncertainties due to momentum scale calibration and the energy loss correction are fully correlated between the two measurements, while all other uncertainties are fully uncorrelated, one obtains

$$[m(\Omega_b^-) - m(\Xi_b^-)]_{\mathrm{LHCb\ comb}} = 248.50 \pm 0.51\,(\mathrm{stat}) \pm 0.37\,(\mathrm{syst})\,\mathrm{MeV}/c^2. \qquad (2)$$

In order to obtain the combination of LHCb determinations of the Ω_b^- baryon mass, the measurement in Ref. [7], which does not use the Ξ_b^- mass as a reference, is combined with the two measurements that rely on the Ξ_b^- mass (Ref. [6] and the measurement presented here), which are already combined in Eq. 2. This is achieved by first extracting $m(\Omega_b^-)$ from Eq. (2) using the Ξ_b^- mass value from Ref. [36]. The obtained value of $m(\Omega_b^-)$ is then combined with that from Ref. [7].
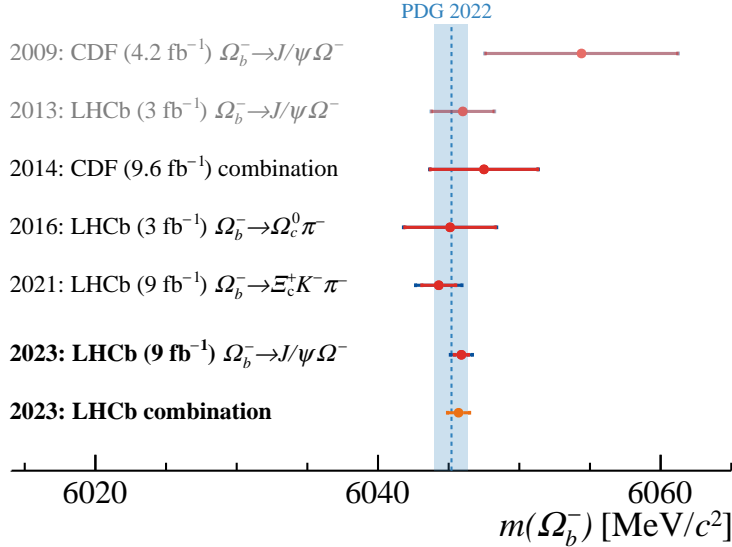
Figure 2: Overview of the Ω_b^- mass measurements to date (red points) [3–7], with corresponding statistical and systematic uncertainties marked in red and blue, respectively, as well as the current world average by the PDG [1] (light-blue band). The superseded measurements are shown with lighter colors. The measurement by the DØ experiment [2] of $6165 \pm 22\,\mathrm{MeV}/c^2$ is not shown, because it is inconsistent with all others and falls outside the range of this plot. The new LHCb combination is presented in orange, where the total uncertainty is shown.

The uncertainties due to the momentum-scale and the energy-loss corrections are treated as fully correlated, and all others as uncorrelated. This leads to an LHCb combination of the Ω_b^- baryon mass of

$$m(\Omega_b^-)_{\mathrm{LHCb\ comb}} = 6045.7 \pm 0.5\,(\mathrm{stat}) \pm 0.6\,(\mathrm{syst})\,\mathrm{MeV}/c^2.$$

A summary of Ω_b^- mass determinations from the CDF and LHCb experiments is presented in Fig. 2.

5   Relative production of Ω_b^- and Ξ_b^- baryons

In the Run 1 dataset, the signal yield of the $\Omega_b^- \to J/\psi\,\Omega^-$ decay is limited, and the downstream tracking efficiency is poorly known. Therefore, the relative production ratio of Ω_b^- and Ξ_b^- baryons is only reported at a center-of-mass energy of 13 TeV, using the Run 2 dataset. The relative production ratio of the Ω_b^- and Ξ_b^- baryons, defined in Eq. (1), is experimentally measured using the observed yields (N) of the considered decays, corrected for efficiency (ϵ) and branching fractions ($\mathcal{B}$) of hyperon decays:

$$R = \frac{N(\Omega_b^- \to J/\psi\,\Omega^-)}{N(\Xi_b^- \to J/\psi\,\Xi^-)} \times \frac{\epsilon(\Xi_b^- \to J/\psi\,\Xi^-)}{\epsilon(\Omega_b^- \to J/\psi\,\Omega^-)} \times \frac{\mathcal{B}(\Xi^- \to \Lambda\pi^-)}{\mathcal{B}(\Omega^- \to \Lambda K^-)}. \tag{3}$$

Since the decays $\Lambda \to p\pi^-$ and $J/\psi \to \mu^+\mu^-$ enter both b-baryon decay chains, their branching fractions cancel in the ratio. The world-average values of $\mathcal{B}(\Omega^- \to \Lambda K^-) = (67.8 \pm 0.7)\%$ and $\mathcal{B}(\Xi^- \to \Lambda\pi^-) = (99.887 \pm 0.035)\%$ are used [1]. The efficiencies are

estimated using the relevant simulation samples. In the ratio, many sources of inefficiency and associated systematic uncertainties cancel due to the very similar kinematics and topologies of the two decay modes. However, this cancellation is not expected for the detector acceptance and reconstruction efficiencies due to the large difference in lifetimes between the Ω^- and Ξ^- hyperons.

A simultaneous fit to the Run 2 datasets for both decay modes is performed. The fit setup is nearly identical to that used for the mass measurement, but the signal yield of the $\Omega_b^- \to J/\psi\Omega^-$ decays is expressed as a product of the relative production ratio R, the yield of $\Xi_b^- \to J/\psi\Xi^-$ decays and the ratio of efficiencies for the two decay modes. The mass projections of the fit are shown in Fig. 3.

To determine the ratio in Eq. (3), the ratio of efficiencies is evaluated from calibrated simulation samples of the two signal decays. The calibration procedure is performed to correct for known sources of mismodeling in simulation. The simulated kinematics of b baryons are calibrated by weighting the distribution of the transverse momenta of the Ω_b^- and Ξ_b^- baryons to match their distributions in data, after the background contribution is subtracted using the $_s\mathcal{P}lot$ method [37]. The momentum asymmetries, $(p_1 - p_2)/(p_1 + p_2)$, of the decay products of the Ξ^- and Λ hyperons are calibrated with a similar approach. For the Ω^--hyperon decay, a reasonable agreement is observed between simulation and data, and therefore no weighting is applied. Such a calibration of the momentum asymmetry can account for the simplified modeling of the angular distributions in the simulation of the b-baryon decays according to available phase space. The hardware trigger response is calibrated based on a tag-and-probe approach using $B^+ \to J/\psi K^+$ decays [38]. The muon identification response is calibrated with dedicated tag-and-probe $J/\psi \to \mu^+\mu^-$ samples [39]. After calibration, good agreement between the simulation and background-subtracted data is observed in variables that describe the decay kinematics
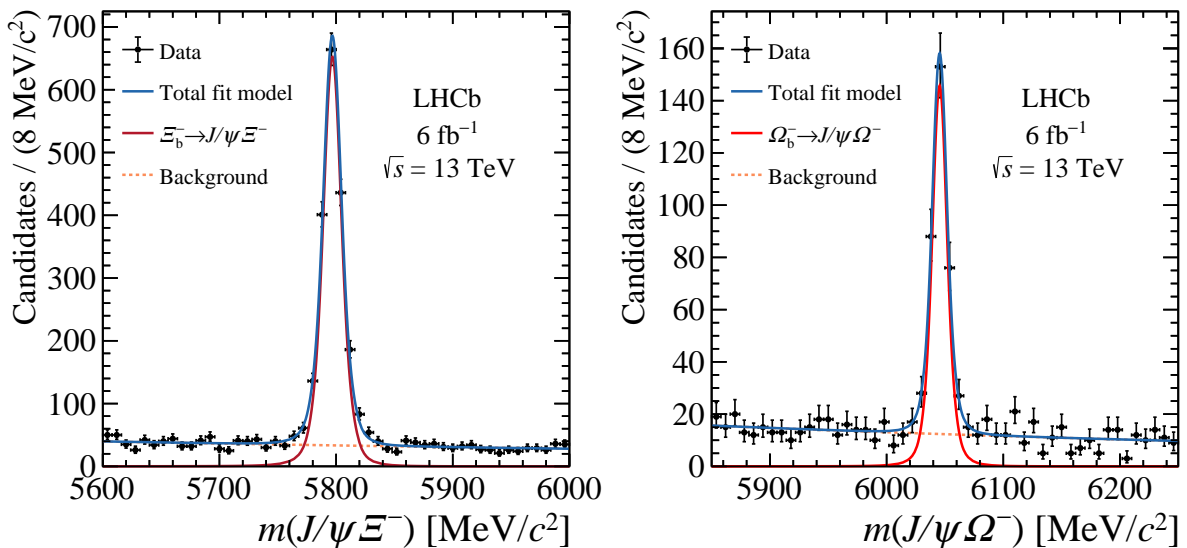
Figure 3: Invariant-mass distributions in the (left) $\Xi_b^- \to J/\psi\Xi^-$ and (right) $\Omega_b^- \to J/\psi\Omega^-$ Run 2 datasets with the results of the simultaneous fit overlaid used for the relative production estimation. In the $\Omega_b^- \to J/\psi\Omega^-$ dataset a Ξ^- mass veto is applied rather than the kaon identification requirement.

Table 3: Efficiencies obtained from the simulated samples of $\Omega_b^- \to J/\psi\Omega^-$ and $\Xi_b^- \to J/\psi\Xi^-$ decays in Run 2, used to extract the ratio R. The uncertainties shown in this table only account for the size of the simulated samples.

Channel	Efficiency
$\Xi_b^- \to J/\psi\Xi^-$	$(0.923 \pm 0.002) \times 10^{-3}$
$\Omega_b^- \to J/\psi\Omega^-$	$(2.065 \pm 0.004) \times 10^{-3}$
ratio Ω_b^-/Ξ_b^-	2.236 ± 0.007

and topology.

The calibrated simulation is used to calculate the signal efficiencies. These efficiencies account for the detector acceptance, the detection, reconstruction, trigger and muon identification efficiency as well as the final kinematic and geometric selection. The resulting efficiencies and their ratio are summarized in Table 3. These efficiency values are found to be higher for the Ω_b^- decay channel, which is mainly attributed to the shorter lifetime of the Ω^- hyperon as compared to the Ξ^- hyperon. This results in a larger fraction of the Ω_b^- decays occurring within the acceptance of the LHCb tracking system.

Using the efficiency ratio from Table 3, the relative production ratio is determined to be $R = 0.120 \pm 0.008$, where the uncertainty is statistical only. The stability of this result is tested with a dataset-splitting procedure similar to that used in the mass measurement. The obtained results for all subsets are in excellent agreement with the baseline result. As an additional test, the ratio is also extracted with the invariant-mass range in the fit reduced by 50 or $100\,\mathrm{MeV}/c^2$ on both sides, yielding a result consistent with the default value.

Possible sources of systematic uncertainty are studied in detail and summarized in Table 4. The size of the simulated samples, used to estimate the signal efficiencies, leads to a 0.3% relative uncertainty on the efficiency ratio. However, the amount of background-subtracted data used to determine the simulation-calibration weights is rather small, especially for the Ω_b^- decay. The systematic uncertainty associated to this limited amount of data is propagated using a bootstrapping technique [40]. All the data candidates used for the determination of the calibration weights are assigned a Poisson-distributed weight of unity mean. This entire calibration procedure is repeated 100 times, resulting in 100

Table 4: Relative systematic uncertainties on R.

Source	Uncertainty [%]
Size of simulated samples	0.3
Calibration of simulation	5.5
Selection criteria	0.1
Lifetimes of b baryons	3.1
Material interactions	0.7
Fit model	0.8
External input ($\mathcal{B}$)	1.0
Total	6.5

alternative efficiency-ratio values. Their RMS leads to a relative systematic uncertainty of 3.9%. Furthermore, alternative binning schemes are tested for the calibration weights on the simulation. For instance, the kinematics of the Ξ_b^- baryon is alternatively calibrated in two dimensions, $p_T(\Xi_b^-) : \eta(\Xi_b^-)$, rather than the default calibration of $p_T(\Xi_b^-)$ alone. For the Ω_b^- baryon, the available amount of data is too small to perform the same two-dimensional calibration. In addition, a correction for the residual data-simulation discrepancies, present after the application of the default calibration chain, was applied, and the associated shift in the final result is treated as another source of systematic uncertainty. A further source of uncertainty originates from imprecise modeling of the downstream tracking efficiency in simulation. To exclude a momentum-dependent bias, the result is tested as a function of the Ξ^- (Ω^-) momentum, and the observed variation (2.8%) is assigned as a systematic uncertainty. A dedicated systematic uncertainty is also assigned for the calibration procedure of the muon identification efficiency in simulation (0.6%) [41]. Overall, the systematic uncertainty related to the calibration of the simulation is found to be 5.5%.

The efficiency of the Ξ^- veto can be incorrectly estimated in simulation if the invariant-mass resolution is not well modeled. This is tested by broadening and narrowing the vetoed mass region and probing the shift in the final result. The associated relative uncertainty is estimated to be 0.1%.

A further uncertainty arises from propagating the uncertainties on the known values of the Ω_b^- and Ξ_b^- baryon lifetimes [1], and is determined by weighting the decay-time distributions in the simulation samples with a dedicated exponential factor. This results in a 3.1% relative uncertainty on the production ratio, due to the relatively poor knowledge of the Ω_b^- baryon lifetime.

Long-lived hyperons can interact with the detector material prior to their decay. The rate of these interactions is not precisely modeled in simulation, due to poor knowledge of the cross-sections for hyperons. A dedicated systematic uncertainty is assigned by comparing the hyperon material-interaction probability estimated with two different versions of the GEANT4 simulation toolkit[2], which use different values for hadronic interaction cross-sections, amounting to a relative uncertainty of 0.7%.

Several sources of systematic uncertainty related to the fit model are considered. Using pseudoexperiments, the uncertainties related to fit bias and the chosen signal and background models are studied. The final relative systematic uncertainty from the fit model is 0.8%. Lastly, the uncertainties on the branching fractions of the $\Omega^- \to \Lambda K^-$ and $\Xi^- \to \Lambda \pi^-$ decays are propagated to the final result, leading to a relative uncertainty of 1.0%.

Accounting for the fit result and the systematic uncertainties, the ratio R is measured to be:

$$R = 0.120 \pm 0.008\,(\text{stat}) \pm 0.008\,(\text{syst}),$$

in the kinematic region $2 < \eta < 6$ and $p_T < 20$ GeV/c for the Ξ_b^- and Ω_b^- baryons. Although the ratio of production cross-sections between the Ω_b^- and Ξ_b^- is not expected to match between the two production environments, a comparison can be useful. This result is lower than, but consistent with the value measured by the CDF experiment in $p\bar{p}$ collisions at the center-of-mass energy of 1.96 TeV, $R = 0.27 \pm 0.12\,(\text{stat}) \pm 0.01\,(\text{syst})$ [3].

---

[2]The GEANT4 versions used are `v9r6p4` and `v10r6p2`.

This comparison is limited by the very low signal yield of $\Omega_b^- \to J/\psi\Omega^-$ decays in the CDF dataset.

The CDF measurement was reinterpreted, using the predicted value of the branching fraction of the Ω_b^- decay, to extract an Ω_b^- production fraction of $f_{\Omega_b^-} \sim 0.5 \times 10^{-2}$ at the Tevatron [14]. Similarly, one can estimate the value of $f_{\Omega_b^-}/f_{\Xi_b^-}$ at LHCb using the predictions for the relevant branching fractions. For instance, Ref. [14] predicts $\mathcal{B}(\Omega_b^- \to J/\psi\Omega^-) = (5.3^{+5.0}_{-3.4}) \times 10^{-4}$ and quotes $\mathcal{B}(\Xi_b^- \to J/\psi\Xi^-) = (5.1 \pm 3.2) \times 10^{-4}$. As the ratio of these two branching fractions is close to unity, the resulting value of $f_{\Omega_b^-}/f_{\Xi_b^-}$ is about 0.12. However, it should be noted that other predictions of the two branching fractions [12–14] would yield different results.

6 Conclusion

The mass difference between the Ω_b^- and Ξ_b^- baryons is measured to be

$$m(\Omega_b^-) - m(\Xi_b^-) = 248.54 \pm 0.51\,(\text{stat}) \pm 0.38\,(\text{syst})\,\text{MeV}/c^2$$

using an LHCb dataset corresponding to an intergrated luminosity of $9\,\text{fb}^{-1}$. This result is consistent with the previous direct determination of this quantity in Ref. [6], $m(\Omega_b^-) - m(\Xi_b^-) = 247.4 \pm 3.2 \pm 0.5\,\text{MeV}/c^2$, which uses LHCb data of b-baryon decays to open-charm final states collected at the center-of-mass energies of 7 and 8 TeV. The combination of the two results is

$$[m(\Omega_b^-) - m(\Xi_b^-)]_{\text{LHCb comb}} = 248.50 \pm 0.51\,(\text{stat}) \pm 0.37\,(\text{syst})\,\text{MeV}/c^2.$$

The value of the Ω_b^- baryon mass is measured to be

$$m(\Omega_b^-) = 6045.9 \pm 0.5\,(\text{stat}) \pm 0.6\,(\text{syst})\,\text{MeV}/c^2,$$

where the value of $m(\Xi_b^-) = 5797.33 \pm 0.24 \pm 0.29\,\text{MeV}/c^2$ from Ref. [36] is used as a reference. This measurement represents the most precise determination of the Ω_b^--baryon mass, and is consistent with the current world average of $6045.2 \pm 1.2\,\text{MeV}/c^2$ [1]. It supersedes the value measured in Ref. [4].

The combination of the $m(\Omega_b^-)$ value determined in this paper with the previous LHCb measurements in Refs. [6,7] leads to

$$m(\Omega_b^-)_{\text{LHCb comb}} = 6045.7 \pm 0.5\,(\text{stat}) \pm 0.6\,(\text{syst})\,\text{MeV}/c^2.$$

In addition, the relative production rate of the Ω_b^- to Ξ_b^- baryons multiplied by the branching fractions of their decays to $J/\psi\Omega^-$ and $J/\psi\Xi^-$ final states is reported for the first time at the LHC. In pp collisions at a center-of-mass energy of 13 TeV, and for b baryons with $2 < \eta < 6$ and $p_{\text{T}} < 20$ GeV/c, this ratio is determined to be

$$R = 0.120 \pm 0.008\,(\text{stat}) \pm 0.008\,(\text{syst}).$$

This measurement is lower than, but still in agreement with the value measured by the CDF experiment in $p\bar{p}$ collisions at a center-of-mass energy of 1.96 TeV [3]. This new measurement allows for a more precise determination of the total b-quark production cross-section at the LHC. Further theoretical studies of the branching fractions of the decays $\Omega_b^- \to J/\psi\Omega^-$ and $\Xi_b^- \to J/\psi\Xi^-$ are needed in order to interpret this result in terms of $f_{\Omega_b^-}/f_{\Xi_b^-}$.

Acknowledgements

References

[1] Particle Data Group, R. L. Workman *et al.*, *Review of particle physics*, Prog. Theor. Exp. Phys. **2022** (2022) 083C01.

[2] DØ collaboration, V. M. Abazov *et al.*, *Observation of the doubly strange b baryon* Ω_b^-, Phys. Rev. Lett. **101** (2008) 232002, arXiv:0808.4142.

[3] CDF collaboration, T. Aaltonen *et al.*, *Observation of the* Ω_b^- *baryon and measurement of the properties of the* Ξ_b^- *and* Ω_b^- *baryons*, Phys. Rev. **D80** (2009) 072003, arXiv:0905.3123.

[4] LHCb collaboration, R. Aaij *et al.*, *Measurements of the* Λ_b^0, Ξ_b^-, *and* Ω_b^- *baryon masses*, Phys. Rev. Lett. **110** (2013) 182001, arXiv:1302.1072.

[5] CDF collaboration, T. A. Aaltonen *et al.*, *Mass and lifetime measurements of bottom and charm baryons in* $p\bar{p}$ *collisions at* $\sqrt{s} = 1.96$ *TeV*, Phys. Rev. **D89** (2014) 072014, arXiv:1403.8126.

[6] LHCb collaboration, R. Aaij *et al.*, *Measurements of the mass and lifetime of the* Ω_b^- *baryon*, Phys. Rev. **D93** (2016) 092007, arXiv:1604.01412.

[7] LHCb collaboration, R. Aaij *et al.*, *Observation of excited* Ω_c^0 *baryons in* $\Omega_b^- \to \Xi_c^+ K^- \pi^+$ *decays*, Phys. Rev. **D104** (2021) L091102, arXiv:2107.03419.

[8] LHCb collaboration, R. Aaij *et al.*, *Measurement of the b-quark production cross-section in* 7 *and* 13 *TeV pp collisions*, Phys. Rev. Lett. **118** (2017) 052002, Erratum ibid. **119** (2017) 169901, arXiv:1612.05140.
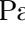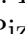
[9] LHCb collaboration, R. Aaij *et al.*, *Measurement of b-hadron fractions in 13 TeV pp collisions*, Phys. Rev. **D100** (2019) 031102(R), `arXiv:1902.06794`.

[10] LHCb collaboration, R. Aaij *et al.*, *Measurement of the Ω_c^0 lifetime*, Phys. Rev. Lett. **121** (2018) 092003, `arXiv:1807.02024`.

[11] LHCb collaboration, R. Aaij *et al.*, *Measurement of the mass and production rate of Ξ_b^- baryons*, Phys. Rev. **D99** (2019) 052006, `arXiv:1901.07075`.

[12] H.-Y. Cheng, *Nonleptonic weak decays of bottom baryons*, Phys. Rev. **D56** (1997) 2799, `arXiv:hep-ph/9612223`, [Erratum: Phys.Rev.D 99, 079901 (2019)].

[13] T. Gutsche, M. A. Ivanov, J. G. Körner, and V. E. Lyubovitskij, *Nonleptonic two-body decays of single heavy baryons Λ_Q, Ξ_Q, and Ω_Q (Q = b, c) induced by W emission in the covariant confined quark model*, Phys. Rev. **D98** (2018) 074011, `arXiv:1806.11549`.

[14] Y.-K. Hsiao and C.-C. Lih, *Fragmentation fraction $f_{\Omega_b^-}$ and the $\Omega_b^- \to \Omega^- J/\psi$ decay in the light-front formalism*, Phys. Rev. **D105** (2022) 056015, `arXiv:2110.00945`.

[15] LHCb collaboration, A. A. Alves Jr. *et al.*, *The LHCb detector at the LHC*, JINST **3** (2008) S08005.

[16] LHCb collaboration, R. Aaij *et al.*, *LHCb detector performance*, Int. J. Mod. Phys. **A30** (2015) 1530022, `arXiv:1412.6352`.

[17] R. Aaij *et al.*, *Performance of the LHCb Vertex Locator*, JINST **9** (2014) P09007, `arXiv:1405.7808`.

[18] R. Arink *et al.*, *Performance of the LHCb Outer Tracker*, JINST **9** (2014) P01002, `arXiv:1311.3893`.

[19] P. d'Argent *et al.*, *Improved performance of the LHCb Outer Tracker in LHC Run 2*, JINST **12** (2017) P11016, `arXiv:1708.00819`.

[20] M. Adinolfi *et al.*, *Performance of the LHCb RICH detector at the LHC*, Eur. Phys. J. **C73** (2013) 2431, `arXiv:1211.6759`.

[21] A. A. Alves Jr. *et al.*, *Performance of the LHCb muon system*, JINST **8** (2013) P02022, `arXiv:1211.1346`.

[22] R. Aaij *et al.*, *The LHCb trigger and its performance in 2011*, JINST **8** (2013) P04022, `arXiv:1211.3055`.

[23] LHCb collaboration, R. Aaij *et al.*, *Precision measurement of D meson mass differences*, JHEP **06** (2013) 065, `arXiv:1304.6865`.

[24] T. Sjöstrand, S. Mrenna, and P. Skands, *A brief introduction to PYTHIA 8.1*, Comput. Phys. Commun. **178** (2008) 852, `arXiv:0710.3820`; T. Sjöstrand, S. Mrenna, and P. Skands, *PYTHIA 6.4 physics and manual*, JHEP **05** (2006) 026, `arXiv:hep-ph/0603175`.
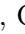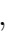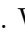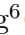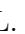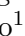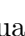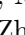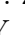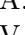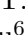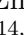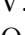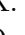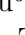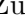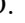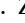
[25] I. Belyaev *et al.*, *Handling of the generation of primary events in Gauss, the LHCb simulation framework*, J. Phys. Conf. Ser. **331** (2011) 032047.

[26] D. J. Lange, *The EvtGen particle decay simulation package*, Nucl. Instrum. Meth. **A462** (2001) 152.

[27] N. Davidson, T. Przedzinski, and Z. Was, *PHOTOS interface in C++: Technical and physics documentation*, Comp. Phys. Comm. **199** (2016) 86, `arXiv:1011.0937`.

[28] Geant4 collaboration, J. Allison *et al.*, *Geant4 developments and applications*, IEEE Trans. Nucl. Sci. **53** (2006) 270; Geant4 collaboration, S. Agostinelli *et al.*, *Geant4: A simulation toolkit*, Nucl. Instrum. Meth. **A506** (2003) 250.

[29] M. Clemencic *et al.*, *The LHCb simulation application, Gauss: Design, evolution and experience*, J. Phys. Conf. Ser. **331** (2011) 032023.

[30] L. Oliver, J.-C. Raynal, and R. Sinha, *Note on new interesting baryon channels to measure the photon polarization in $b \to s\gamma$*, Phys. Rev. **D82** (2010) 117502, `arXiv:1007.3632`.

[31] M.-S. Liu, K.-L. Wang, Q.-F. Lü, and X.-H. Zhong, *Ω baryon spectrum and their decays in a constituent quark model*, Phys. Rev. **D101** (2020) 016002, `arXiv:1910.10322`.

[32] W. D. Hulsbergen, *Decay chain fitting with a Kalman filter*, Nucl. Instrum. Meth. **A552** (2005) 566, `arXiv:physics/0503191`.

[33] W. Verkerke and D. P. Kirkby, *The RooFit toolkit for data modeling*, eConf **C0303241** (2003) MOLT007, `arXiv:physics/0306116`.

[34] R. Brun and F. Rademakers, *ROOT: An object oriented data analysis framework*, Nucl. Instrum. Meth. **A389** (1997) 81.

[35] T. Skwarnicki, *A study of the radiative cascade transitions between the Upsilon-prime and Upsilon resonances*, PhD thesis, Institute of Nuclear Physics, Krakow, 1986, DESY-F31-86-02.

[36] LHCb collaboration, R. Aaij *et al.*, *Observation of a new Ξ_b^0 state*, Phys. Rev. **D103** (2021) 012004, `arXiv:2010.14485`.

[37] M. Pivk and F. R. Le Diberder, *sPlot: A statistical tool to unfold data distributions*, Nucl. Instrum. Meth. **A555** (2005) 356, `arXiv:physics/0402083`.

[38] S. Tolk, J. Albrecht, F. Dettori, and A. Pellegrino, *Data driven trigger efficiency determination at LHCb*, LHCb-PUB-2014-039, 2014.

[39] R. Aaij *et al.*, *Selection and processing of calibration samples to measure the particle identification performance of the LHCb experiment in Run 2*, Eur. Phys. J. Tech. Instr. **6** (2019) 1, `arXiv:1803.00824`.

[40] B. Efron, *Bootstrap methods: Another look at the jackknife*, Ann. Statist. **7** (1979) 1.

[41] L. Anderlini *et al.*, *The PIDCalib package*, LHCb-PUB-2016-021, 2016.

LHCb collaboration

R. Aaij[32] , A.S.W. Abdelmotteleb[51] , C. Abellan Beteta[45], F. Abudinén[51] ,
T. Ackernley[55] , B. Adeva[41] , M. Adinolfi[49] , P. Adlarson[77] , H. Afsharnia[9],
C. Agapopoulou[13] , C.A. Aidala[78] , Z. Ajaltouni[9], S. Akar[60] , K. Akiba[32] ,
P. Albicocco[23] , J. Albrecht[15] , F. Alessio[43] , M. Alexander[54] , A. Alfonso Albero[40] ,
Z. Aliouche[57] , P. Alvarez Cartelle[50] , R. Amalric[13] , S. Amato[2] , J.L. Amey[49] ,
Y. Amhis[11,43] , L. An[43] , L. Anderlini[22] , M. Andersson[45] , A. Andreianov[38] ,
M. Andreotti[21] , D. Andreou[63] , D. Ao[6] , F. Archilli[31,t] , A. Artamonov[38] ,
M. Artuso[63] , E. Aslanides[10] , M. Atzeni[45] , B. Audurier[12] , I.B Bachiller Perea[8] ,
S. Bachmann[17] , M. Bachmayer[44] , J.J. Back[51] , A. Bailly-reyre[13],
P. Baladron Rodriguez[41] , V. Balagura[12] , W. Baldini[21,43] , J. Baptista de Souza Leite[1] ,
M. Barbetti[22,j] , R.J. Barlow[57] , S. Barsuk[11] , W. Barter[53] , M. Bartolini[50] ,
F. Baryshnikov[38] , J.M. Basels[14] , G. Bassi[29,q] , B. Batsukh[4] , A. Battig[15] ,
A. Bay[44] , A. Beck[51] , M. Becker[15] , F. Bedeschi[29] , I.B. Bediaga[1] , A. Beiter[63],
S. Belin[41] , V. Bellee[45] , K. Belous[38] , I. Belov[38] , I. Belyaev[38] , G. Benane[10] ,
G. Bencivenni[23] , E. Ben-Haim[13] , A. Berezhnoy[38] , R. Bernet[45] , S. Bernet Andres[39] ,
D. Berninghoff[17], H.C. Bernstein[63], C. Bertella[57] , A. Bertolin[28] , C. Betancourt[45] ,
F. Betti[43] , Ia. Bezshyiko[45] , J. Bhom[35] , L. Bian[69] , M.S. Bieker[15] , N.V. Biesuz[21] ,
P. Billoir[13] , A. Biolchini[32] , M. Birch[56] , F.C.R. Bishop[50] , A. Bitadze[57] ,
A. Bizzeti , M.P. Blago[50] , T. Blake[51] , F. Blanc[44] , J.E. Blank[15] , S. Blusk[63] ,
D. Bobulska[54] , V.B Bocharnikov[38] , J.A. Boelhauve[15] , O. Boente Garcia[12] ,
T. Boettcher[60] , A. Boldyrev[38] , C.S. Bolognani[75] , R. Bolzonella[21,i] , N. Bondar[38,43] ,
F. Borgato[28] , S. Borghi[57] , M. Borsato[17] , J.T. Borsuk[35] , S.A. Bouchiba[44] ,
T.J.V. Bowcock[55] , A. Boyer[43] , C. Bozzi[21] , M.J. Bradley[56], S. Braun[61] ,
A. Brea Rodriguez[41] , N. Breer[15] , J. Brodzicka[35] , A. Brossa Gonzalo[41] , J. Brown[55] ,
D. Brundu[27] , A. Buonaura[45] , L. Buonincontri[28] , A.T. Burke[57] , C. Burr[43] ,
A. Bursche[67], A. Butkevich[38] , J.S. Butter[32] , J. Buytaert[43] , W. Byczynski[43] ,
S. Cadeddu[27] , H. Cai[69], R. Calabrese[21,i] , L. Calefice[15] , S. Cali[23] , M. Calvi[26,m] ,
M. Calvo Gomez[39] , P. Campana[23] , D.H. Campora Perez[75] ,
A.F. Campoverde Quezada[6] , S. Capelli[26,m] , L. Capriotti[20] , A. Carbone[20,g] ,
R. Cardinale[24,k] , A. Cardini[27] , P. Carniti[26,m] , L. Carus[14], A. Casais Vidal[41] ,
R. Caspary[17] , G. Casse[55] , M. Cattaneo[43] , G. Cavallero[21] , V. Cavallini[21,i] ,
S. Celani[44] , J. Cerasoli[10] , D. Cervenkov[58] , A.J. Chadwick[55] , I. Chahrour[78] ,
M.G. Chapman[49], M. Charles[13] , Ph. Charpentier[43] , C.A. Chavez Barajas[55] ,
M. Chefdeville[8] , C. Chen[10] , S. Chen[4] , A. Chernov[35] , S. Chernyshenko[47] ,
V. Chobanova[41] , S. Cholak[44] , M. Chrzaszcz[35] , A. Chubykin[38] , V. Chulikov[38] ,
P. Ciambrone[23] , M.F. Cicala[51] , X. Cid Vidal[41] , G. Ciezarek[43] , P. Cifra[43] ,
G. Ciullo[i,21] , P.E.L. Clarke[53] , M. Clemencic[43] , H.V. Cliff[50] , J. Closier[43] ,
J.L. Cobbledick[57] , V. Coco[43] , J. Cogan[10] , E. Cogneras[9] , L. Cojocariu[37] ,
P. Collins[43] , T. Colombo[43] , L. Congedo[19] , A. Contu[27] , N. Cooke[48] ,
I. Corredoira [41] , G. Corti[43] , B. Couturier[43] , D.C. Craik[45] , M. Cruz Torres[1,e] ,
R. Currie[53] , C.L. Da Silva[62] , S. Dadabaev[38] , L. Dai[66] , X. Dai[5] , E. Dall'Occo[15] ,
J. Dalseno[41] , C. D'Ambrosio[43] , J. Daniel[9] , A. Danilina[38] , P. d'Argent[19] ,
J.E. Davies[57] , A. Davis[57] , O. De Aguiar Francisco[57] , J. de Boer[43] , K. De Bruyn[74] ,
S. De Capua[57] , M. De Cian[44] , U. De Freitas Carneiro Da Graca[1] , E. De Lucia[23] ,
J.M. De Miranda[1] , L. De Paula[2] , M. De Serio[19,f] , D. De Simone[45] , P. De Simone[23] ,
F. De Vellis[15] , J.A. de Vries[75] , C.T. Dean[62] , F. Debernardis[19,f] , D. Decamp[8] ,
V. Dedu[10] , L. Del Buono[13] , B. Delaney[59] , H.-P. Dembinski[15] , V. Denysenko[45] ,
O. Deschamps[9] , F. Dettori[27,h] , B. Dey[72] , P. Di Nezza[23] , I. Diachkov[38] ,

S. Didenko[38] (iD), L. Dieste Maronas[41], S. Ding[63] (iD), V. Dobishuk[47] (iD), A. Dolmatov[38],
C. Dong[3] (iD), A.M. Donohoe[18] (iD), F. Dordei[27] (iD), A.C. dos Reis[1] (iD), L. Douglas[54],
A.G. Downes[8] (iD), P. Duda[76] (iD), M.W. Dudek[35] (iD), L. Dufour[43] (iD), V. Duk[73] (iD), P. Durante[43] (iD),
M. M. Duras[76] (iD), J.M. Durham[62] (iD), D. Dutta[57] (iD), A. Dziurda[35] (iD), A. Dzyuba[38] (iD),
S. Easo[52] (iD), U. Egede[64] (iD), A. Egorychev[38] (iD), V. Egorychev[38] (iD), C. Eirea Orro[41],
S. Eisenhardt[53] (iD), E. Ejopu[57] (iD), S. Ek-In[44] (iD), L. Eklund[77] (iD), M.E Elashri[60] (iD),
J. Ellbracht[15] (iD), S. Ely[56] (iD), A. Ene[37] (iD), E. Epple[60] (iD), S. Escher[14] (iD), J. Eschle[45] (iD),
S. Esen[45] (iD), T. Evans[57] (iD), F. Fabiano[27,h] (iD), L.N. Falcao[1] (iD), Y. Fan[6] (iD), B. Fang[11,69] (iD),
L. Fantini[73,p] (iD), M. Faria[44] (iD), S. Farry[55] (iD), D. Fazzini[26,m] (iD), L.F Felkowski[76] (iD), M. Feo[43] (iD),
M. Fernandez Gomez[41] (iD), A.D. Fernez[61] (iD), F. Ferrari[20] (iD), L. Ferreira Lopes[44] (iD),
F. Ferreira Rodrigues[2] (iD), S. Ferreres Sole[32] (iD), M. Ferrillo[45] (iD), M. Ferro-Luzzi[43] (iD),
S. Filippov[38] (iD), R.A. Fini[19] (iD), M. Fiorini[21,i] (iD), M. Firlej[34] (iD), K.M. Fischer[58] (iD),
D.S. Fitzgerald[78] (iD), C. Fitzpatrick[57] (iD), T. Fiutowski[34] (iD), F. Fleuret[12] (iD), M. Fontana[20] (iD),
F. Fontanelli[24,k] (iD), R. Forty[43] (iD), D. Foulds-Holt[50] (iD), V. Franco Lima[55] (iD),
M. Franco Sevilla[61] (iD), M. Frank[43] (iD), E. Franzoso[21,i] (iD), G. Frau[17] (iD), C. Frei[43] (iD),
D.A. Friday[57] (iD), L.F Frontini[25,l] (iD), J. Fu[6] (iD), Q. Fuehring[15] (iD), T. Fulghesu[13] (iD),
E. Gabriel[32] (iD), G. Galati[19,f] (iD), M.D. Galati[32] (iD), A. Gallas Torreira[41] (iD), D. Galli[20,g] (iD),
S. Gambetta[53,43] (iD), M. Gandelman[2] (iD), P. Gandini[25] (iD), H.G Gao[6] (iD), R. Gao[58] (iD), Y. Gao[7] (iD),
Y. Gao[5] (iD), M. Garau[27,h] (iD), L.M. Garcia Martin[51] (iD), P. Garcia Moreno[40] (iD),
J. García Pardiñas[43] (iD), B. Garcia Plana[41], F.A. Garcia Rosales[12] (iD), L. Garrido[40] (iD),
C. Gaspar[43] (iD), R.E. Geertsema[32] (iD), D. Gerick[17], L.L. Gerken[15] (iD), E. Gersabeck[57] (iD),
M. Gersabeck[57] (iD), T. Gershon[51] (iD), L. Giambastiani[28] (iD), V. Gibson[50] (iD), H.K. Giemza[36] (iD),
A.L. Gilman[58] (iD), M. Giovannetti[23] (iD), A. Gioventù[41] (iD), P. Gironella Gironell[40] (iD),
C. Giugliano[21,i] (iD), M.A. Giza[35] (iD), K. Gizdov[53] (iD), E.L. Gkougkousis[43] (iD), V.V. Gligorov[13,43] (iD),
C. Göbel[65] (iD), E. Golobardes[39] (iD), D. Golubkov[38] (iD), A. Golutvin[56,38] (iD), A. Gomes[1,a] (iD),
S. Gomez Fernandez[40] (iD), F. Goncalves Abrantes[58] (iD), M. Goncerz[35] (iD), G. Gong[3] (iD),
I.V. Gorelov[38] (iD), C. Gotti[26] (iD), J.P. Grabowski[71] (iD), T. Grammatico[13] (iD),
L.A. Granado Cardoso[43] (iD), E. Graugés[40] (iD), E. Graverini[44] (iD), G. Graziani (iD), A. T. Grecu[37] (iD),
L.M. Greeven[32] (iD), N.A. Grieser[60] (iD), L. Grillo[54] (iD), S. Gromov[38] (iD), B.R. Gruberg Cazon[58] (iD),
C. Gu[3] (iD), M. Guarise[21,i] (iD), M. Guittiere[11] (iD), P. A. Günther[17] (iD), A.K. Guseinov[38] (iD),
E. Gushchin[38] (iD), A. Guth[14], Y. Guz[5,38,43] (iD), T. Gys[43] (iD), T. Hadavizadeh[64] (iD),
C. Hadjivasiliou[61] (iD), G. Haefeli[44] (iD), C. Haen[43] (iD), J. Haimberger[43] (iD), S.C. Haines[50] (iD),
T. Halewood-leagas[55] (iD), M.M. Halvorsen[43] (iD), P.M. Hamilton[61] (iD), J. Hammerich[55] (iD),
Q. Han[7] (iD), X. Han[17] (iD), S. Hansmann-Menzemer[17] (iD), L. Hao[6] (iD), N. Harnew[58] (iD),
T. Harrison[55] (iD), C. Hasse[43] (iD), M. Hatch[43] (iD), J. He[6,c] (iD), K. Heijhoff[32] (iD), F.H Hemmer[43] (iD),
C. Henderson[60] (iD), R.D.L. Henderson[64,51] (iD), A.M. Hennequin[59] (iD), K. Hennessy[55] (iD),
L. Henry[43] (iD), J. Herd[56] (iD), J. Heuel[14] (iD), A. Hicheur[2] (iD), D. Hill[44] (iD), M. Hilton[57] (iD),
S.E. Hollitt[15] (iD), J. Horswill[57] (iD), R. Hou[7] (iD), Y. Hou[8] (iD), J. Hu[17], J. Hu[67] (iD), W. Hu[5] (iD),
X. Hu[3] (iD), W. Huang[6] (iD), X. Huang[69], W. Hulsbergen[32] (iD), R.J. Hunter[51] (iD), M. Hushchyn[38] (iD),
D. Hutchcroft[55] (iD), P. Ibis[15] (iD), M. Idzik[34] (iD), D. Ilin[38] (iD), P. Ilten[60] (iD), A. Inglessi[38] (iD),
A. Iniukhin[38] (iD), A. Ishteev[38] (iD), K. Ivshin[38] (iD), R. Jacobsson[43] (iD), H. Jage[14] (iD),
S.J. Jaimes Elles[42] (iD), S. Jakobsen[43] (iD), E. Jans[32] (iD), B.K. Jashal[42] (iD), A. Jawahery[61] (iD),
V. Jevtic[15] (iD), E. Jiang[61] (iD), X. Jiang[4,6] (iD), Y. Jiang[6] (iD), M. John[58] (iD), D. Johnson[59] (iD),
C.R. Jones[50] (iD), T.P. Jones[51] (iD), S.J Joshi[36] (iD), B. Jost[43] (iD), N. Jurik[43] (iD), I. Juszczak[35] (iD),
S. Kandybei[46] (iD), Y. Kang[3] (iD), M. Karacson[43] (iD), D. Karpenkov[38] (iD), M. Karpov[38] (iD),
J.W. Kautz[60] (iD), F. Keizer[43] (iD), D.M. Keller[63] (iD), M. Kenzie[51] (iD), T. Ketel[32] (iD), B. Khanji[63] (iD),
A. Kharisova[38] (iD), S. Kholodenko[38] (iD), G. Khreich[11] (iD), T. Kirn[14] (iD), V.S. Kirsebom[44] (iD),
O. Kitouni[59] (iD), S. Klaver[33] (iD), N. Kleijne[29,q] (iD), K. Klimaszewski[36] (iD), M.R. Kmiec[36] (iD),
S. Koliiev[47] (iD), L. Kolk[15] (iD), A. Kondybayeva[38] (iD), A. Konoplyannikov[38] (iD), P. Kopciewicz[34] (iD),
R. Kopecna[17], P. Koppenburg[32] (iD), M. Korolev[38] (iD), I. Kostiuk[32] (iD), O. Kot[47],

18

S. Kotriakhova [iD], A. Kozachuk[38] [iD], P. Kravchenko[38] [iD], L. Kravchuk[38] [iD], M. Kreps[51] [iD],
S. Kretzschmar[14] [iD], P. Krokovny[38] [iD], W. Krupa[34] [iD], W. Krzemien[36] [iD], J. Kubat[17],
S. Kubis[76] [iD], W. Kucewicz[35] [iD], M. Kucharczyk[35] [iD], V. Kudryavtsev[38] [iD], E.K Kulikova[38] [iD],
A. Kupsc[77] [iD], D. Lacarrere[43] [iD], G. Lafferty[57] [iD], A. Lai[27] [iD], A. Lampis[27,h] [iD],
D. Lancierini[45] [iD], C. Landesa Gomez[41] [iD], J.J. Lane[57] [iD], R. Lane[49] [iD], C. Langenbruch[14] [iD],
J. Langer[15] [iD], O. Lantwin[38] [iD], T. Latham[51] [iD], F. Lazzari[29,r] [iD], C. Lazzeroni[48] [iD],
R. Le Gac[10] [iD], S.H. Lee[78] [iD], R. Lefèvre[9] [iD], A. Leflat[38] [iD], S. Legotin[38] [iD], P. Lenisa[i,21] [iD],
O. Leroy[10] [iD], T. Lesiak[35] [iD], B. Leverington[17] [iD], A. Li[3] [iD], H. Li[67] [iD], K. Li[7] [iD], P. Li[43] [iD],
P.-R. Li[68] [iD], S. Li[7] [iD], T. Li[4] [iD], T. Li[67] [iD], Y. Li[4] [iD], Z. Li[63] [iD], X. Liang[63] [iD], C. Lin[6] [iD],
T. Lin[52] [iD], R. Lindner[43] [iD], V. Lisovskyi[15] [iD], R. Litvinov[27,h] [iD], G. Liu[67] [iD], H. Liu[6] [iD],
K. Liu[68] [iD], Q. Liu[6] [iD], S. Liu[4,6] [iD], A. Lobo Salvia[40] [iD], A. Loi[27] [iD], R. Lollini[73] [iD],
J. Lomba Castro[41] [iD], I. Longstaff[54], J.H. Lopes[2] [iD], A. Lopez Huertas[40] [iD],
S. López Soliño[41] [iD], G.H. Lovell[50] [iD], Y. Lu[4,b] [iD], C. Lucarelli[22,j] [iD], D. Lucchesi[28,o] [iD],
S. Luchuk[38] [iD], M. Lucio Martinez[75] [iD], V. Lukashenko[32,47] [iD], Y. Luo[3] [iD], A. Lupato[57] [iD],
E. Luppi[21,i] [iD], A. Lusiani[29,q] [iD], K. Lynch[18] [iD], X.-R. Lyu[6] [iD], R. Ma[6] [iD], S. Maccolini[15] [iD],
F. Machefert[11] [iD], F. Maciuc[37] [iD], I. Mackay[58] [iD], V. Macko[44] [iD], L.R. Madhan Mohan[50] [iD],
A. Maevskiy[38] [iD], D. Maisuzenko[38] [iD], M.W. Majewski[34], J.J. Malczewski[35] [iD], S. Malde[58] [iD],
B. Malecki[35,43] [iD], A. Malinin[38] [iD], T. Maltsev[38] [iD], G. Manca[27,h] [iD], G. Mancinelli[10] [iD],
C. Mancuso[11,25,l] [iD], R. Manera Escalero[40], D. Manuzzi[20] [iD], C.A. Manzari[45] [iD],
D. Marangotto[25,l] [iD], J.F. Marchand[8] [iD], U. Marconi[20] [iD], S. Mariani[43] [iD], C. Marin Benito[40] [iD],
J. Marks[17] [iD], A.M. Marshall[49] [iD], P.J. Marshall[55], G. Martelli[73,p] [iD], G. Martellotti[30] [iD],
L. Martinazzoli[43,m] [iD], M. Martinelli[26,m] [iD], D. Martinez Santos[41] [iD], F. Martinez Vidal[42] [iD],
A. Massafferri[1] [iD], M. Materok[14] [iD], R. Matev[43] [iD], A. Mathad[45] [iD], V. Matiunin[38] [iD],
C. Matteuzzi[26] [iD], K.R. Mattioli[12] [iD], A. Mauri[56] [iD], E. Maurice[12] [iD], J. Mauricio[40] [iD],
M. Mazurek[43] [iD], M. McCann[56] [iD], L. Mcconnell[18] [iD], T.H. McGrath[57] [iD], N.T. McHugh[54] [iD],
A. McNab[57] [iD], R. McNulty[18] [iD], B. Meadows[60] [iD], G. Meier[15] [iD], D. Melnychuk[36] [iD],
S. Meloni[26,m] [iD], M. Merk[32,75] [iD], A. Merli[25,l] [iD], L. Meyer Garcia[2] [iD], D. Miao[4,6] [iD],
H. Miao[6] [iD], M. Mikhasenko[71,d] [iD], D.A. Milanes[70] [iD], E. Millard[51], M. Milovanovic[43] [iD],
M.-N. Minard[8,†], A. Minotti[26,m] [iD], E. Minucci[63] [iD], T. Miralles[9] [iD], S.E. Mitchell[53] [iD],
B. Mitreska[15] [iD], D.S. Mitzel[15] [iD], A. Modak[52] [iD], A. Mödden[15] [iD], R.A. Mohammed[58] [iD],
R.D. Moise[14] [iD], S. Mokhnenko[38] [iD], T. Mombächer[41] [iD], M. Monk[51,64] [iD], I.A. Monroy[70] [iD],
S. Monteil[9] [iD], G. Morello[23] [iD], M.J. Morello[29,q] [iD], M.P. Morgenthaler[17] [iD], J. Moron[34] [iD],
A.B. Morris[43] [iD], A.G. Morris[10] [iD], R. Mountain[63] [iD], H. Mu[3] [iD], E. Muhammad[51] [iD],
F. Muheim[53] [iD], M. Mulder[74] [iD], K. Müller[45] [iD], C.H. Murphy[58] [iD], D. Murray[57] [iD],
R. Murta[56] [iD], P. Muzzetto[27,h] [iD], P. Naik[49] [iD], T. Nakada[44] [iD], R. Nandakumar[52] [iD],
T. Nanut[43] [iD], I. Nasteva[2] [iD], M. Needham[53] [iD], N. Neri[25,l] [iD], S. Neubert[71] [iD], N. Neufeld[43] [iD],
P. Neustroev[38], R. Newcombe[56], J. Nicolini[15,11] [iD], D. Nicotra[75] [iD], E.M. Niel[44] [iD],
S. Nieswand[14], N. Nikitin[38] [iD], N.S. Nolte[59] [iD], C. Normand[8,h,27] [iD], J. Novoa Fernandez[41] [iD],
G.N Nowak[60] [iD], C. Nunez[78] [iD], A. Oblakowska-Mucha[34] [iD], V. Obraztsov[38] [iD], T. Oeser[14] [iD],
S. Okamura[21,i] [iD], R. Oldeman[27,h] [iD], F. Oliva[53] [iD], C.J.G. Onderwater[74] [iD], R.H. O'Neil[53] [iD],
J.M. Otalora Goicochea[2] [iD], T. Ovsiannikova[38] [iD], P. Owen[45] [iD], A. Oyanguren[42] [iD],
O. Ozcelik[53] [iD], K.O. Padeken[71] [iD], B. Pagare[51] [iD], P.R. Pais[43] [iD], T. Pajero[58] [iD],
A. Palano[19] [iD], M. Palutan[23] [iD], G. Panshin[38] [iD], L. Paolucci[51] [iD], A. Papanestis[52] [iD],
M. Pappagallo[19,f] [iD], L.L. Pappalardo[21,i] [iD], C. Pappenheimer[60] [iD], W. Parker[61] [iD],
C. Parkes[57] [iD], B. Passalacqua[21] [iD], G. Passaleva[22] [iD], A. Pastore[19] [iD], M. Patel[56] [iD],
C. Patrignani[20,g] [iD], C.J. Pawley[75] [iD], A. Pellegrino[32] [iD], M. Pepe Altarelli[43] [iD],
S. Perazzini[20] [iD], D. Pereima[38] [iD], A. Pereiro Castro[41] [iD], P. Perret[9] [iD], K. Petridis[49] [iD],
A. Petrolini[24,k] [iD], S. Petrucci[53] [iD], M. Petruzzo[25] [iD], H. Pham[63] [iD], A. Philippov[38] [iD],
R. Piandani[6] [iD], L. Pica[29,q] [iD], M. Piccini[73] [iD], B. Pietrzyk[8] [iD], G. Pietrzyk[11] [iD], M. Pili[58] [iD],
D. Pinci[30] [iD], F. Pisani[43] [iD], M. Pizzichemi[26,m,43] [iD], V. Placinta[37] [iD], J. Plews[48] [iD],

M. Plo Casasus[41] , F. Polci[13,43] , M. Poli Lener[23] , A. Poluektov[10] , N. Polukhina[38] ,
I. Polyakov[43] , E. Polycarpo[2] , S. Ponce[43] , D. Popov[6,43] , S. Poslavskii[38] ,
K. Prasanth[35] , L. Promberger[17] , C. Prouve[41] , V. Pugatch[47] , V. Puill[11] ,
G. Punzi[29,r] , H.R. Qi[3] , W. Qian[6] , N. Qin[3] , S. Qu[3] , R. Quagliani[44] ,
N.V. Raab[18] , B. Rachwal[34] , J.H. Rademacker[49] , R. Rajagopalan[63], M. Rama[29] ,
M. Ramos Pernas[51] , M.S. Rangel[2] , F. Ratnikov[38] , G. Raven[33] ,
M. Rebollo De Miguel[42] , F. Redi[43] , J. Reich[49] , F. Reiss[57] , C. Remon Alepuz[42],
Z. Ren[3] , P.K. Resmi[58] , R. Ribatti[29,q] , A.M. Ricci[27] , S. Ricciardi[52] ,
K. Richardson[59] , M. Richardson-Slipper[53] , K. Rinnert[55] , P. Robbe[11] ,
G. Robertson[53] , E. Rodrigues[55,43] , E. Rodriguez Fernandez[41] , J.A. Rodriguez Lopez[70] ,
E. Rodriguez Rodriguez[41] , D.L. Rolf[43] , A. Rollings[58] , P. Roloff[43] ,
V. Romanovskiy[38] , M. Romero Lamas[41] , A. Romero Vidal[41] , M. Rotondo[23] ,
M.S. Rudolph[63] , T. Ruf[43] , R.A. Ruiz Fernandez[41] , J. Ruiz Vidal[42], A. Ryzhikov[38] ,
J. Ryzka[34] , J.J. Saborido Silva[41] , N. Sagidova[38] , N. Sahoo[48] , B. Saitta[27,h] ,
M. Salomoni[43] , C. Sanchez Gras[32] , I. Sanderswood[42] , R. Santacesaria[30] ,
C. Santamarina Rios[41] , M. Santimaria[23] , L. Santoro[1] , E. Santovetti[31,t] ,
D. Saranin[38] , G. Sarpis[53] , M. Sarpis[71] , A. Sarti[30] , C. Satriano[30,s] , A. Satta[31] ,
M. Saur[5] , D. Savrina[38] , H. Sazak[9] , L.G. Scantlebury Smead[58] , A. Scarabotto[13] ,
S. Schael[14] , S. Scherl[55] , A. M. Schertz[72] , M. Schiller[54] , H. Schindler[43] ,
M. Schmelling[16] , B. Schmidt[43] , S. Schmitt[14] , O. Schneider[44] , A. Schopper[43] ,
M. Schubiger[32] , N. Schulte[15] , S. Schulte[44] , M.H. Schune[11] , R. Schwemmer[43] ,
B. Sciascia[23] , A. Sciuccati[43] , S. Sellam[41] , A. Semennikov[38] , M. Senghi Soares[33] ,
A. Sergi[24,k] , N. Serra[45] , L. Sestini[28] , A. Seuthe[15] , Y. Shang[5] , D.M. Shangase[78] ,
M. Shapkin[38] , I. Shchemerov[38] , L. Shchutska[44] , T. Shears[55] , L. Shekhtman[38] ,
Z. Shen[5] , S. Sheng[4,6] , V. Shevchenko[38] , B. Shi[6] , E.B. Shields[26,m] , Y. Shimizu[11] ,
E. Shmanin[38] , R. Shorkin[38] , J.D. Shupperd[63] , B.G. Siddi[21,i] , R. Silva Coutinho[63] ,
G. Simi[28] , S. Simone[19,f] , M. Singla[64] , N. Skidmore[57] , R. Skuza[17] ,
T. Skwarnicki[63] , M.W. Slater[48] , J.C. Smallwood[58] , J.G. Smeaton[50] , E. Smith[45] ,
K. Smith[62] , M. Smith[56] , A. Snoch[32] , L. Soares Lavra[9] , M.D. Sokoloff[60] ,
F.J.P. Soler[54] , A. Solomin[38,49] , A. Solovev[38] , I. Solovyev[38] , R. Song[64] ,
F.L. Souza De Almeida[2] , B. Souza De Paula[2] , E. Spadaro Norella[25,l] , E. Spedicato[20] ,
J.G. Speer[15] , E. Spiridenkov[38], P. Spradlin[54] , V. Sriskaran[43] , F. Stagni[43] ,
M. Stahl[43] , S. Stahl[43] , S. Stanislaus[58] , E.N. Stein[43] , O. Steinkamp[45] ,
O. Stenyakin[38], H. Stevens[15] , D. Strekalina[38] , Y.S Su[6] , F. Suljik[58] , J. Sun[27] ,
L. Sun[69] , Y. Sun[61] , P.N. Swallow[48] , K. Swientek[34] , A. Szabelski[36] , T. Szumlak[34] ,
M. Szymanski[43] , Y. Tan[3] , S. Taneja[57] , M.D. Tat[58] , A. Terentev[45] , F. Teubert[43] ,
E. Thomas[43] , D.J.D. Thompson[48] , H. Tilquin[56] , V. Tisserand[9] , S. T'Jampens[8] ,
M. Tobin[4] , L. Tomassetti[21,i] , G. Tonani[25,l] , X. Tong[5] , D. Torres Machado[1] ,
D.Y. Tou[3] , C. Trippl[44] , G. Tuci[6] , N. Tuning[32] , A. Ukleja[36] , D.J. Unverzagt[17] ,
A. Usachov[33] , A. Ustyuzhanin[38] , U. Uwer[17] , V. Vagnoni[20] , A. Valassi[43] ,
G. Valenti[20] , N. Valls Canudas[39] , M. Van Dijk[44] , H. Van Hecke[62] ,
E. van Herwijnen[56] , C.B. Van Hulse[41,v] , M. van Veghel[32] , R. Vazquez Gomez[40] ,
P. Vazquez Regueiro[41] , C. Vázquez Sierra[41] , S. Vecchi[21] , J.J. Velthuis[49] ,
M. Veltri[22,u] , A. Venkateswaran[44] , M. Veronesi[32] , M. Vesterinen[51] , D. Vieira[60] ,
M. Vieites Diaz[44] , X. Vilasis-Cardona[39] , E. Vilella Figueras[55] , A. Villa[20] ,
P. Vincent[13] , F.C. Volle[11] , D. vom Bruch[10] , V. Vorobyev[38], N. Voropaev[38] ,
K. Vos[75] , C. Vrahas[53] , J. Walsh[29] , E.J. Walton[64] , G. Wan[5] , C. Wang[17] ,
G. Wang[7] , J. Wang[5] , J. Wang[4] , J. Wang[3] , J. Wang[69] , M. Wang[25] , R. Wang[49] ,
X. Wang[67] , Y. Wang[7] , Z. Wang[45] , Z. Wang[3] , Z. Wang[6] , J.A. Ward[51,64] ,
N.K. Watson[48] , D. Websdale[56] , Y. Wei[5] , B.D.C. Westhenry[49] , D.J. White[57] ,

M. Whitehead[54] , A.R. Wiederhold[51] , D. Wiedner[15] , G. Wilkinson[58] ,
M.K. Wilkinson[60] , I. Williams[50], M. Williams[59] , M.R.J. Williams[53] , R. Williams[50] ,
F.F. Wilson[52] , W. Wislicki[36] , M. Witek[35] , L. Witola[17] , C.P. Wong[62] ,
G. Wormser[11] , S.A. Wotton[50] , H. Wu[63] , J. Wu[7] , K. Wyllie[43] , Z. Xiang[6] ,
Y. Xie[7] , A. Xu[5] , J. Xu[6] , L. Xu[3] , L. Xu[3] , M. Xu[51] , Q. Xu[6], Z. Xu[9] , Z. Xu[6] ,
D. Yang[3] , S. Yang[6] , X. Yang[5] , Y. Yang[6] , Z. Yang[5] , Z. Yang[61] ,
L.E. Yeomans[55] , V. Yeroshenko[11] , H. Yeung[57] , H. Yin[7] , J. Yu[66] , X. Yuan[63] ,
E. Zaffaroni[44] , M. Zavertyaev[16] , M. Zdybal[35] , M. Zeng[3] , C. Zhang[5] , D. Zhang[7] ,
J. Zhang[6] , L. Zhang[3] , S. Zhang[66] , S. Zhang[5] , Y. Zhang[5] , Y. Zhang[58], Y. Zhao[17] ,
A. Zharkova[38] , A. Zhelezov[17] , Y. Zheng[6] , T. Zhou[5] , X. Zhou[7] , Y. Zhou[6] ,
V. Zhovkovska[11] , X. Zhu[3] , X. Zhu[7] , Z. Zhu[6] , V. Zhukov[14,38] , J. Zhuo[42] ,
Q. Zou[4,6] , S. Zucchelli[20,g] , D. Zuliani[28] , G. Zunica[57] .

[1]Centro Brasileiro de Pesquisas Físicas (CBPF), Rio de Janeiro, Brazil
[2]Universidade Federal do Rio de Janeiro (UFRJ), Rio de Janeiro, Brazil
[3]Center for High Energy Physics, Tsinghua University, Beijing, China
[4]Institute Of High Energy Physics (IHEP), Beijing, China
[5]School of Physics State Key Laboratory of Nuclear Physics and Technology, Peking University, Beijing, China
[6]University of Chinese Academy of Sciences, Beijing, China
[7]Institute of Particle Physics, Central China Normal University, Wuhan, Hubei, China
[8]Université Savoie Mont Blanc, CNRS, IN2P3-LAPP, Annecy, France
[9]Université Clermont Auvergne, CNRS/IN2P3, LPC, Clermont-Ferrand, France
[10]Aix Marseille Univ, CNRS/IN2P3, CPPM, Marseille, France
[11]Université Paris-Saclay, CNRS/IN2P3, IJCLab, Orsay, France
[12]Laboratoire Leprince-Ringuet, CNRS/IN2P3, Ecole Polytechnique, Institut Polytechnique de Paris, Palaiseau, France
[13]LPNHE, Sorbonne Université, Paris Diderot Sorbonne Paris Cité, CNRS/IN2P3, Paris, France
[14]I. Physikalisches Institut, RWTH Aachen University, Aachen, Germany
[15]Fakultät Physik, Technische Universität Dortmund, Dortmund, Germany
[16]Max-Planck-Institut für Kernphysik (MPIK), Heidelberg, Germany
[17]Physikalisches Institut, Ruprecht-Karls-Universität Heidelberg, Heidelberg, Germany
[18]School of Physics, University College Dublin, Dublin, Ireland
[19]INFN Sezione di Bari, Bari, Italy
[20]INFN Sezione di Bologna, Bologna, Italy
[21]INFN Sezione di Ferrara, Ferrara, Italy
[22]INFN Sezione di Firenze, Firenze, Italy
[23]INFN Laboratori Nazionali di Frascati, Frascati, Italy
[24]INFN Sezione di Genova, Genova, Italy
[25]INFN Sezione di Milano, Milano, Italy
[26]INFN Sezione di Milano-Bicocca, Milano, Italy
[27]INFN Sezione di Cagliari, Monserrato, Italy
[28]Università degli Studi di Padova, Università e INFN, Padova, Padova, Italy
[29]INFN Sezione di Pisa, Pisa, Italy
[30]INFN Sezione di Roma La Sapienza, Roma, Italy
[31]INFN Sezione di Roma Tor Vergata, Roma, Italy
[32]Nikhef National Institute for Subatomic Physics, Amsterdam, Netherlands
[33]Nikhef National Institute for Subatomic Physics and VU University Amsterdam, Amsterdam, Netherlands
[34]AGH - University of Science and Technology, Faculty of Physics and Applied Computer Science, Kraków, Poland
[35]Henryk Niewodniczanski Institute of Nuclear Physics Polish Academy of Sciences, Kraków, Poland
[36]National Center for Nuclear Research (NCBJ), Warsaw, Poland
[37]Horia Hulubei National Institute of Physics and Nuclear Engineering, Bucharest-Magurele, Romania
[38]Affiliated with an institute covered by a cooperation agreement with CERN

^{39}DS4DS, La Salle, Universitat Ramon Llull, Barcelona, Spain

^{40}ICCUB, Universitat de Barcelona, Barcelona, Spain

^{41}Instituto Galego de Física de Altas Enerxías (IGFAE), Universidade de Santiago de Compostela, Santiago de Compostela, Spain

^{42}Instituto de Fisica Corpuscular, Centro Mixto Universidad de Valencia - CSIC, Valencia, Spain

^{43}European Organization for Nuclear Research (CERN), Geneva, Switzerland

^{44}Institute of Physics, Ecole Polytechnique Fédérale de Lausanne (EPFL), Lausanne, Switzerland

^{45}Physik-Institut, Universität Zürich, Zürich, Switzerland

^{46}NSC Kharkiv Institute of Physics and Technology (NSC KIPT), Kharkiv, Ukraine

^{47}Institute for Nuclear Research of the National Academy of Sciences (KINR), Kyiv, Ukraine

^{48}University of Birmingham, Birmingham, United Kingdom

^{49}H.H. Wills Physics Laboratory, University of Bristol, Bristol, United Kingdom

^{50}Cavendish Laboratory, University of Cambridge, Cambridge, United Kingdom

^{51}Department of Physics, University of Warwick, Coventry, United Kingdom

^{52}STFC Rutherford Appleton Laboratory, Didcot, United Kingdom

^{53}School of Physics and Astronomy, University of Edinburgh, Edinburgh, United Kingdom

^{54}School of Physics and Astronomy, University of Glasgow, Glasgow, United Kingdom

^{55}Oliver Lodge Laboratory, University of Liverpool, Liverpool, United Kingdom

^{56}Imperial College London, London, United Kingdom

^{57}Department of Physics and Astronomy, University of Manchester, Manchester, United Kingdom

^{58}Department of Physics, University of Oxford, Oxford, United Kingdom

^{59}Massachusetts Institute of Technology, Cambridge, MA, United States

^{60}University of Cincinnati, Cincinnati, OH, United States

^{61}University of Maryland, College Park, MD, United States

^{62}Los Alamos National Laboratory (LANL), Los Alamos, NM, United States

^{63}Syracuse University, Syracuse, NY, United States

^{64}School of Physics and Astronomy, Monash University, Melbourne, Australia, associated to ^{51}

^{65}Pontifícia Universidade Católica do Rio de Janeiro (PUC-Rio), Rio de Janeiro, Brazil, associated to ^{2}

^{66}Physics and Micro Electronic College, Hunan University, Changsha City, China, associated to ^{7}

^{67}Guangdong Provincial Key Laboratory of Nuclear Science, Guangdong-Hong Kong Joint Laboratory of Quantum Matter, Institute of Quantum Matter, South China Normal University, Guangzhou, China, associated to ^{3}

^{68}Lanzhou University, Lanzhou, China, associated to ^{4}

^{69}School of Physics and Technology, Wuhan University, Wuhan, China, associated to ^{3}

^{70}Departamento de Fisica , Universidad Nacional de Colombia, Bogota, Colombia, associated to ^{13}

^{71}Universität Bonn - Helmholtz-Institut für Strahlen und Kernphysik, Bonn, Germany, associated to ^{17}

^{72}Eotvos Lorand University, Budapest, Hungary, associated to ^{43}

^{73}INFN Sezione di Perugia, Perugia, Italy, associated to ^{21}

^{74}Van Swinderen Institute, University of Groningen, Groningen, Netherlands, associated to ^{32}

^{75}Universiteit Maastricht, Maastricht, Netherlands, associated to ^{32}

^{76}Faculty of Material Engineering and Physics, Cracow, Poland, associated to ^{35}

^{77}Department of Physics and Astronomy, Uppsala University, Uppsala, Sweden, associated to ^{54}

^{78}University of Michigan, Ann Arbor, MI, United States, associated to ^{63}

^{a}Universidade de Brasília, Brasília, Brazil

^{b}Central South U., Changsha, China

^{c}Hangzhou Institute for Advanced Study, UCAS, Hangzhou, China

^{d}Excellence Cluster ORIGINS, Munich, Germany

^{e}Universidad Nacional Autónoma de Honduras, Tegucigalpa, Honduras

^{f}Università di Bari, Bari, Italy

^{g}Università di Bologna, Bologna, Italy

^{h}Università di Cagliari, Cagliari, Italy

^{i}Università di Ferrara, Ferrara, Italy

^{j}Università di Firenze, Firenze, Italy

^{k}Università di Genova, Genova, Italy

^{l}Università degli Studi di Milano, Milano, Italy

^{m}Università di Milano Bicocca, Milano, Italy

[n] *Università di Modena e Reggio Emilia, Modena, Italy*
[o] *Università di Padova, Padova, Italy*
[p] *Università di Perugia, Perugia, Italy*
[q] *Scuola Normale Superiore, Pisa, Italy*
[r] *Università di Pisa, Pisa, Italy*
[s] *Università della Basilicata, Potenza, Italy*
[t] *Università di Roma Tor Vergata, Roma, Italy*
[u] *Università di Urbino, Urbino, Italy*
[v] *Universidad de Alcalá, Alcalá de Henares , Spain*

[†] *Deceased*